International Journal of Innovative Research and Scientific Studies, 8(6) 2025, pages: 2448-2467

IJIRSS
International Journal of Innovative Research & Scientific Studies

ISSN: 2617-6548

URL: www.ijirss.com

Study of the dynamic influence of vertical vibrations of rolling stock on the railway track

Erlan Askenov[1], Aldabergen Bektilevov[1*], Dias Seidemetov[1], Aliya Izbairova[1], Arailym Tursynbayeva[1]

[1]*School of transport engineering and logistics named after M. Tynyshpayev, Satbayev University, Almaty, Kazakhstan.*

Corresponding author: Aldabergen Bektilevov (*Email: Aldabergen_bektilevov@mail.ru*)

Abstract

The results of a theoretical study of the vertical impact of multiaxial locomotives on the track based on the wave theory of elastic deformation propagation are presented. Theoretical and practical problems of dynamic characteristics research at the design stage of modernization of new and existing rail vehicles. Consideration of the impact of compliance with standards on the impact on railway tracks. These issues in the context of crews can be successfully solved using modern methods of analysis and synthesis of dynamic systems. Calculations and practical experiments using modern computer and recording equipment are widely used for dynamic systems. Keywords. Carriage-path, vertical impact of multi-axle locomotives on the track, speed increase, models for analyzing indicators of dynamic qualities of locomotives during vertical fluctuations.

Keywords: Carriage–track, Dynamic characteristics, Kz4A locomotive, Numerical simulation, Rail deflection, VL-80 locomotive.

DOI: 10.53894/ijirss.v8i6.10126
Funding: This study received no specific financial support.
History: Received: 28 July 2025 / **Revised:** 1 September 2025 / **Accepted:** 3 September 2025 / **Published:** 19 September 2025

Competing Interests: The authors declare that they have no competing interests.
Authors' Contributions: All authors contributed equally to the conception and design of the study. All authors have read and agreed to the published version of the manuscript.
Transparency: The authors confirm that the manuscript is an honest, accurate, and transparent account of the study; that no vital features of the study have been omitted; and that any discrepancies from the study as planned have been explained. This study followed all ethical practices during writing.
Publisher: Innovative Research Publishing

1. Introduction

As is known, the locomotives of the first releases, by analogy with the steam locomotives preceding them, were framed, i.e. all driving wheel sets were located in a common body frame, which perceived vertical and horizontal forces of interaction of wheels with rails, as well as longitudinal forces (traction and braking). In frame locomotives, sliding trolleys were used, which transferred parts of the body weight to the track and reduced the forces of lateral impact of the locomotive with the track when passing curved sections of the railway track. In the future, the need to increase the speeds and capacities of diesel locomotives, as well as improve the conditions for fitting them into curves, led to the appearance of such a structural element of the mechanical part as bogies, on which the body frame rested and had the ability to rotate relative to it. The use of trolleys in the design of the mechanical part of locomotives required solving a number of related technical tasks, the corresponding technical tasks include: supporting the wagon body on trolleys moving relative to the vertical axis, transmitting longitudinal and transverse forces in a state of relative motion of the locomotive body and bogies, connecting bogies to each other to improve driving conditions in curves. Strong train–track coupling (longitudinal, lateral and vertical) may result in enhanced wheel–rail wear, rolling contact fatigue, and infrastructure degradation due to their train–track interactions [1, 2]. As a result, the design of the mechanical part of the rolling stock was supplemented with nodes for supporting the body on the trolley, rotary devices, and a device for connecting trolleys. To reduce the likelihood of wheels boxing, a device was provided to equalize the load between the axles of each moving wheel. Prevents a significant reduction in the vertical load on the front axle of each wheelset, bogies, when the maximum tractive effort is achieved when the locomotive is moving from a stop, the maximum tractive effort is achieved when the locomotive is detached from the rail

The history of the development of Russian railways has been accompanied by constant improvement of the technology of maintenance and repair of locomotives, with priority given to ensuring train safety and improving the qualitative and quantitative performance of locomotives

The efficiency of locomotive operation is determined by quantitative and qualitative indicators. A quantitative indicator of the use of locomotives can be attributed to the total mileage and operating time of the locomotives. A qualitative indicator can be attributed to the average daily mileage and the total percentage of defective locomotives.

The total mileage of locomotives consists of the linear mileage performed during movement on the tracks, and the conditional mileage determined during the operation of locomotives within the stations and depots. The linear mileage of locomotives includes the mileage of locomotives at the head of trains, in single running; in multiple traction; in pushing.

The total operating time of train locomotives includes: the time spent by locomotives in motion, at intermediate stations, on the tracks of the main and reverse depots, and at the changing points of locomotive crews.

The average daily mileage of locomotives shows the number of linear kilometers per day per 1 locomotive of the operated fleet. An increase in the average daily mileage frees up some of the locomotives from operation, increases the productivity of locomotive crews, the profitability of the locomotive industry and the efficiency of the transportation process as a whole.

The qualitative indicators considered include such an indicator as the total percentage of defective locomotives.

1.1. Setting the Task

The percentage of defective locomotives characterizes the technical condition of the locomotive fleet and is determined by the ratio of the average daily number of defective locomotives to the inventory fleet. The percentage of defective locomotives characterizes the technical condition of the locomotive fleet and is determined by the ratio of the average daily number of defective locomotives to the inventory fleet.

The percentage of defective locomotives reflects the condition of the depot's repair base, as well as the degree of reliability of the locomotives.

Reducing the percentage of defective locomotives is provided by:

- Improving the condition of locomotives;
- Improving their operational reliability;
- Reduction of downtime in repairs;
- The introduction of a diagnostic option for the organization of repair production and the improvement of the professional culture of locomotive crews and repair workers.

The experience of operating locomotives shows that the determining factors are the organization of the work of locomotive crews and maintenance workers (Figure 1).

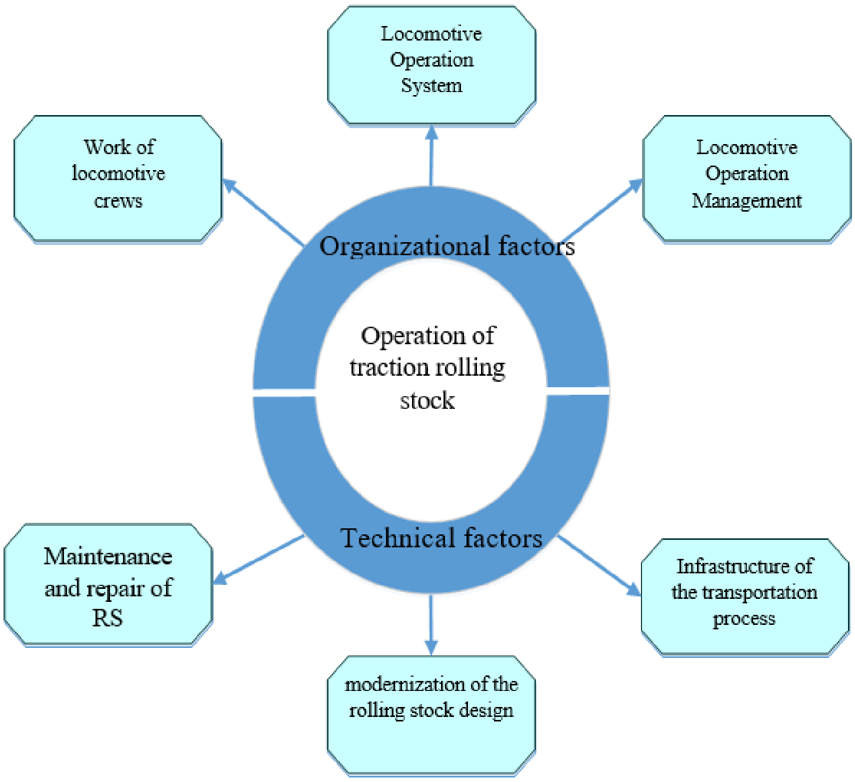

Figure 1.
Technical factors of the transportation process.

1.2. Numerical Modeling Methodology

Not all KZ4A series locomotives were in service during the period under review, as evidenced by the mileage values of the locomotives. (Figure 2). As can be seen from Figure 2, the KZ4A 0005 locomotive has not been in service since 2015-2018, and in 2019 it worked for about 2 days.

In more detail, the efficiency of the KZ4A series locomotives can be estimated by the operating time (Figure 3). As can be seen from Figure 3, the average operating time of locomotives does not exceed 133 days per year (2016). If we take into account that there are 365 days in calendar year 1, then the percentage of working days per year did not exceed 36% of the total number of days per year. that is, 64% of the days of the year the KZ4A series locomotives were idle.

Figure 4 shows information on the percentage of KZ4A series locomotives in the operational and non-operational fleet. In 2022, 3 KZ4A series locomotives were in operation, and in 2023, only two.

As the analysis of the usage indicators of the KZ4A series electric locomotives for 2015-2022 showed, these locomotives are not operated efficiently, they have been in an unused fleet for a long time.

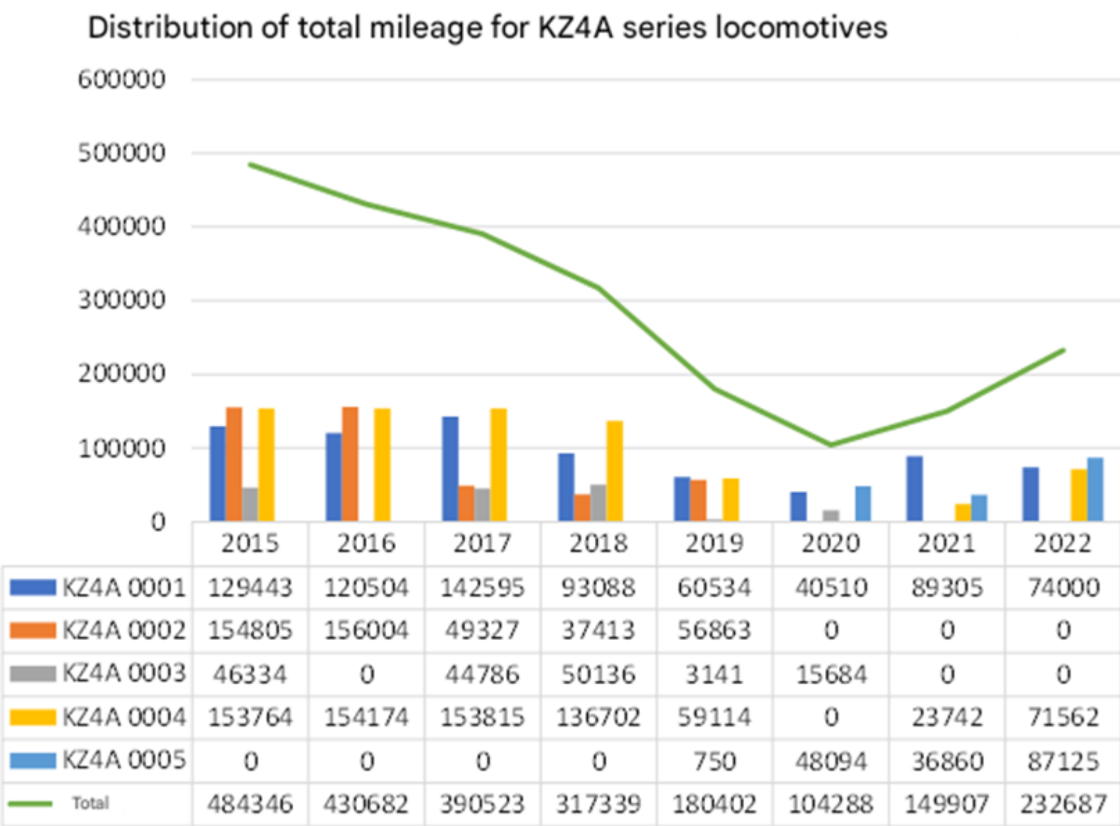

Figure 2.
Mileage of KZ4A series locomotives

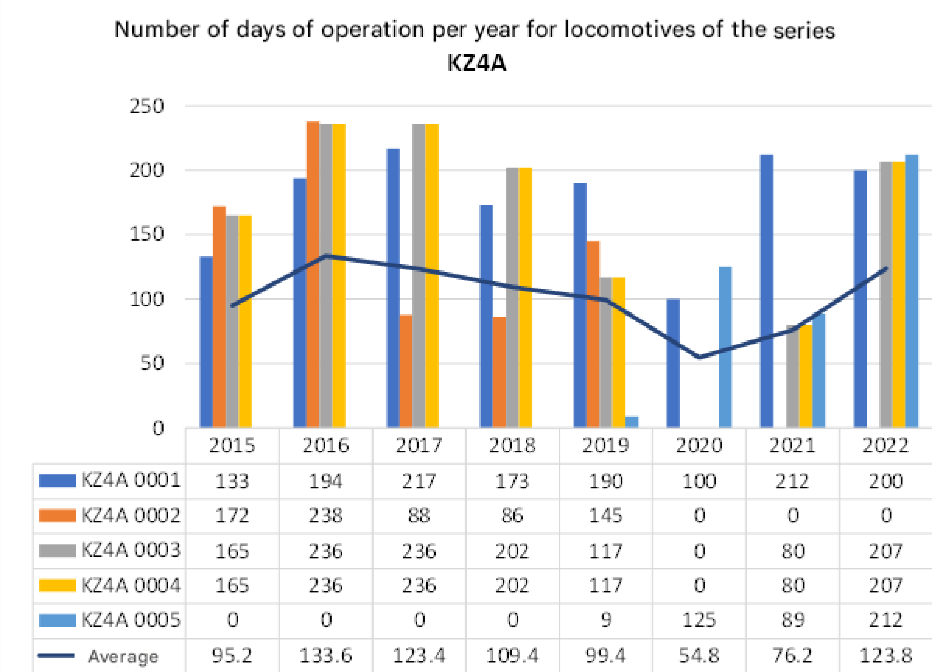

Figure 3.
Number of operating days of KZ4A series locomotives per year

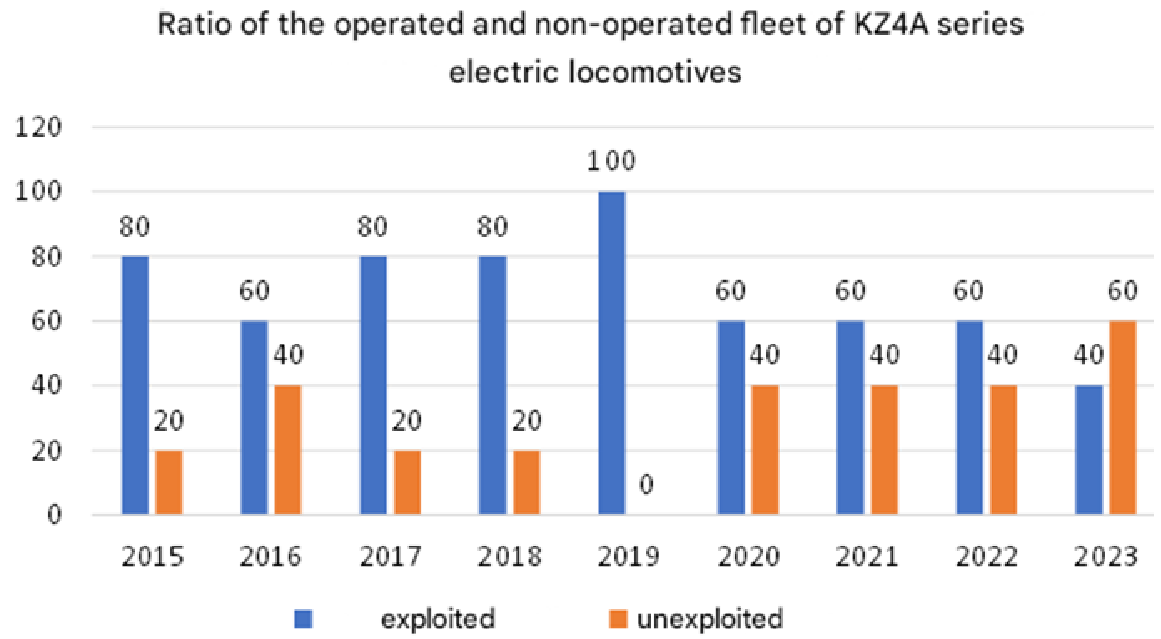

Figure 4.
Percentage of KZ4A series locomotives in the operational and non-operational fleet.

The wave (discrete-continuum) theory of elastic wave propagation is used to model the dynamics of the locomotive and the track [3, 4]. The locomotive is represented by a system of coupled masses: bodies, bogies and wheelsets. The mass intensities and inertial moments of the elements are calculated using the formulas (see Table 1).

Table 1.
The initial data for the calculation.

Title	Designation	Type of electric locomotive	
		VL-80 (ВЛ-80)	**KZ-4A**
Radius of the curve of the track	R, m	600	600
Locomotive base	$l_к$ m	10,5	13,55
The distance between the axes of the couplers of one section	$l_л$, m	15	20,032
The gap between the ridges of the bandages and the head of the outer rail	Δ, mm	10	10
Weight of one section of an electric locomotive	$m_Л$, kg	96000	82000
Body weight	m_K, kg	51000	48000
Unsprung weight of one wheelset	$2q$, kg	6400	3000
Rail mass intensity P65	μ_p, kg /m.	65	65
Maximum speed of movement	$v_к$ km/h	110	160
Number of wheelsets per section	n, pc	4	4

The method of calculating the intensity of mass and the mass moment of inertia of the crew model of electric locomotives type VL-80 and KZ-4A

1.*The intensity of the body mass within the length $l_к$*

$$\mu_K = \frac{m_K}{l_K}.$$

For the VL-80 electric locomotive:

$$\mu_K = \frac{51000}{10,5} = 4857 \text{ kg/m.}$$

For electric locomotive KZ-4A:

$$\mu_K = \frac{48000}{13,54} = 3542,4 \text{ kg/m.}$$

2. *We determine the sprung mass of the two bogies of the electric locomotive:*

$$2m_T = m_Л - m_K - n \cdot 2q .$$

For the VL-80 electric locomotive:

$$2m_T = 92000 - 51000 - 4 \cdot 6400 = 15400 \text{ kg.}$$

For electric locomotive KZ-4A:

$$2m_T = 82000 - 48000 - 4 \cdot 3000 = 22000 \text{ kg.}$$

3. *We determine the intensity of the weight of the trolleys:*

$$\mu_T = \frac{2m_T}{l_K} .$$

For the VL-80 electric locomotive:

$$\mu_T = \frac{15400}{10,5} = 1467 \text{ kg/m.}$$

For electric locomotive KZ-4A:

$$\mu_T = \frac{22000}{13,55} = 1623,6 \text{ kg/m.}$$

4. We determine the intensity of the unsprung mass of the wheelsets:

$$\mu_0 = \frac{n \cdot 2q}{l_к} .$$

For the VL-80 electric locomotive:

$$\mu_0 = \frac{4 * 6400}{10,5} = 2438 \text{ kg/m.}$$

For electric locomotive KZ-4A:

$$\mu_0 = \frac{4 * 3000}{13,55} = 885,6 \text{ kg/m.}$$

5. *We calculate the intensity of the elastic bond between the ridges of the wheelset bands and the head of the outer rail:*

$$K_\Delta = \mu_0 \frac{v_к^2 \cdot 2 \cdot 10^3}{R \cdot \Delta} .$$

For the VL-80 electric locomotive:

$$K_\Delta = 2438 \frac{30^2 \cdot 2 \cdot 10^3}{600 \cdot 10} = 7,31 \cdot 10^5 \text{ N/m}^2.$$

For electric locomotive KZ-4A:

$$K_\Delta = 885,6 \frac{30^2 \cdot 2 \cdot 10^3}{600 \cdot 10} = 2,65 \cdot 10^5 \text{ N/m}^2.$$

5. *We determine the intensity of the elastic bonds of the outer rail with the base of the track:*

$$K_1 = \frac{K_P K_\Delta}{K_P + K_\Delta} .$$

For the VL-80 electric locomotive:

$$K_1 = \frac{2{,}9 \cdot 10^6 \cdot 7{,}31 \cdot 10^5}{2{,}9 \cdot 10^6 + 7{,}31 \cdot 10^5} = 5{,}84 \cdot 10^5 \text{ N/m}^2.$$

For electric locomotive KZ-4A:

$$K_1 = \frac{2{,}28 \cdot 10^6 \cdot 2{,}65 \cdot 10^5}{2{,}28 \cdot 10^6 + 2{,}65 \cdot 10^5} = 2{,}38 \cdot 10^5 \text{ N/m}^2.$$

6. *We determine the equivalent mass intensity of the first model of an "external elastic rail on an elastic base" with the intensity K_1 and unsprung masses of the wheelsets of the electric locomotive model.*

$$\mu_1 = K_1 \left(\frac{m_Л}{2 l_K K_P} + \frac{\mu_0}{K_\Delta} \right).$$

For the VL-80 electric locomotive:

$$\mu_1 = 5{,}84 \cdot 10^5 \cdot \left(\frac{96000}{2 \cdot 10{,}5 \cdot 2{,}9 \cdot 10^6} + \frac{2438}{7{,}31 \cdot 10^5} \right) = 2867 \text{ N/m}^2.$$

For electric locomotive KZ-4A:

$$\mu_1 = 2{,}38 \cdot 10^5 \cdot \left(\frac{82000}{2 \cdot 13{,}55 \cdot 2{,}28 \cdot 10^6} + \frac{885{,}6}{2{,}65 \cdot 10^5} \right) = 1108{,}5 \text{ N/m}^2.$$

7. The intensity of elastic bonds of trolley frames and unsprung masses of wheelsets

$$K_T = \frac{Ж_Г}{l_K}.$$

For the VL-80 electric locomotive:

$$K_T = \frac{128640000}{10{,}5} = 12{,}25 \cdot 10^6 \text{ N/m}^2.$$

For electric locomotive KZ-4A:

$$K_T = \frac{128640000}{13{,}55} = 9{,}5 \cdot 10^6 \text{ N/m}^2.$$

8. *We determine the intensity of the elastic coupling of the second model of "trolley masses with an elastic outer rail and the base of the track"*

$$K_2 = \frac{K_P K_\Delta K_T}{K_P K_\Delta + K_\Delta K_T + K_T K_P}.$$

For the VL-80 electric locomotive:

$$K_2 = \frac{2{,}9 \cdot 10^6 \cdot 7{,}31 \cdot 10^5 \cdot 12{,}25 \cdot 10^6}{2{,}9 \cdot 10^6 \cdot 7{,}31 \cdot 10^5 + 7{,}31 \cdot 10^5 \cdot 12{,}25 \cdot 10^6 + 2{,}9 \cdot 10^6 \cdot 12{,}25 \cdot 10^6} = 5{,}57 \cdot 10^5 \text{ N/m}^2$$

For electric locomotive KZ-4A:

$$K_2 = \frac{2{,}28 \cdot 10^6 \cdot 2{,}65 \cdot 10^5 \cdot 9{,}5 \cdot 10^6}{2{,}28 \cdot 10^6 \cdot 2{,}65 \cdot 10^5 + 2{,}65 \cdot 10^5 \cdot 9{,}5 \cdot 10^6 + 2{,}28 \cdot 10^6 \cdot 9{,}5 \cdot 10^6} = 2{,}32 \cdot 10^5 \text{ N/m}^2.$$

9. The calculation of the reduced intensity of the second model is performed according to the formula:

$$\mu_2 = K_2\left(\frac{\mu_1}{K_1} + \frac{\mu_T}{K_2}\right).$$

For the VL-80 electric locomotive:

$$\mu_2 = 5{,}57 \cdot 10^5 \cdot \left(\frac{2867}{5{,}84 \cdot 10^5} + \frac{1467}{5{,}57 \cdot 10^5}\right) = 4582{,}4 \text{ kg/m.}$$

For electric locomotive KZ-4A:

$$\mu_2 = 2{,}32 \cdot 10^5 \cdot \left(\frac{1108{,}5}{5{,}84 \cdot 10^5} + \frac{1347{,}6}{5{,}57 \cdot 10^5}\right) = 2705{,}5 \text{ kg/m.}$$

10. The intensity of the elastic connections between the mass intensities of the bogies μ_t and the body μ_k of the locomotive

For the VL-80 electric locomotive:

$$K_K = \frac{4{,}3 \cdot 10^6}{10{,}5} = 4{,}1 \cdot 10^5 \text{ N/m}^2.$$

For electric locomotive KZ-4A:

$$K_K = \frac{242400}{13{,}55} = 17{,}9 \cdot 10^3 \text{ N/m}^2.$$

11. We determine the reduced intensity of the elastic coupling of the third model with the rigid base of the track.

$$K_3 = \frac{K_K K_P K_\Delta K_T}{K_P K_\Delta K_K + K_K K_\Delta K_T + K_K K_T K_P + K_P K_\Delta K_T}.$$

For the VL-80 electric locomotive:

$$K_3 = \frac{2{,}9 \cdot 10^6 \cdot 7{,}31 \cdot 10^5 \cdot 12{,}25 \cdot 10^6 \cdot 4{,}1 \cdot 10^5}{2{,}9 \cdot 10^6 \cdot 7{,}31 \cdot 10^5 \cdot 12{,}25 \cdot 10^6 + 2{,}9 \cdot 10^6 \cdot 7{,}31 \cdot 10^5 \cdot 4{,}1 \cdot 10^5} \times$$

$$\times \frac{}{2{,}9 \cdot 10^6 \cdot 12{,}25 \cdot 10^6 \cdot 4{,}1 \cdot 10^5 + 7{,}31 \cdot 10^5 \cdot 12{,}25 \cdot 10^6 \cdot 4{,}1 \cdot 10^5} = 2{,}36 \cdot 10^5,$$

For electric locomotive KZ-4A:

$$K_3 = \frac{2{,}28 \cdot 10^6 \cdot 2{,}65 \cdot 10^5 \cdot 9{,}5 \cdot 10^6 \cdot 17{,}9 \cdot 10^3}{2{,}28 \cdot 10^6 \cdot 2{,}65 \cdot 10^5 \cdot 9{,}5 \cdot 10^6 + 2{,}28 \cdot 10^6 \cdot 2{,}65 \cdot 10^5 \cdot 17{,}9 \cdot 10^3} \times$$

$$\times \frac{}{2{,}28 \cdot 10^6 \cdot 9{,}5 \cdot 10^6 \cdot 17{,}9 \cdot 10^3 + 2{,}65 \cdot 10^5 \cdot 9{,}5 \cdot 10^6 \cdot 17{,}9 \cdot 10^3} = 1{,}66 \cdot 10^4.$$

12. We determine the reduced mass intensity of the third model

$$\mu_3 = K_3\left(\frac{\mu_2}{K_2} + \frac{\mu_K}{K_3}\right).$$

For the VL-80 electric locomotive:

$$\mu_3 = 2{,}36 \cdot 10^5 \cdot \left(\frac{4582{,}4}{5{,}57 \cdot 10^5} + \frac{4857}{2{,}39 \cdot 10^5}\right) = 6738 \text{ kg/m.}$$

For electric locomotive KZ-4A:

$$\mu_3 = 1{,}66 \cdot 10^4 \cdot (\frac{2705{,}5}{2{,}32 \cdot 10^5} + \frac{3542{,}4}{1{,}66 \cdot 10^4}) = 2611 \text{ kg/m.}$$

To determine the intensity i_1 of the mass moment of inertia of the first model, we use assumptions.
On the uniform placement of the intensity of the unsprung mass of the wheelsets within the rail track width S = 1.52 m.
About the placement of 4 concentrated masses of 0.25 μ1 (0.25 m is one-fourth of the model) at a distance:

$$S_1 = \sqrt{0{,}25^2 + 0{,}25 \cdot S^2},$$

from the center of gravity of the model with a length of 1 p.m.

For VL-80 and KZ-4A electric locomotives:

$$S_1 = \sqrt{0{,}25^2 + 0{,}25 \cdot S^2} = 0{,}25 \cdot \sqrt{1 + 1{,}52}^2 = 0{,}455.$$

About using the formula to calculate:

$$i_1 = 0{,}25 \cdot \mu_1 \cdot 4 \cdot S_1{}^2 = \mu_1 \cdot S_1^2.$$

For the VL-80 electric locomotive:

$$i_1 = 2867 \cdot 0{,}455^2 = 593{,}5 \text{ kg*m}$$

For electric locomotive KZ-4A:

$$i_1 = 1108{,}5 \cdot 0{,}455^2 = 230{,}0 \text{ kg*m}$$

To determine the intensity $i2$ of the mass moment of inertia of the second model, we use assumptions similar to paragraph 15 and formulas for calculating were obtained:

$$i_2 = \mu_2 \cdot \sqrt{0{,}25^2 + 0{,}25 \cdot S_2{}^2}.$$

For the VL-80 electric locomotive:

$$i_2 = 4582{,}4 \cdot 0{,}25 \cdot \sqrt{1 + 2{,}116^2} = 2681 \text{ kg*m.}$$

For electric locomotive KZ-4A:

$$i_2 = 2705{,}5 \cdot 0{,}25 \cdot \sqrt{1 + 2{,}116^2} = 1583 \text{ kg*m}$$

The intensity of the mass moment of inertia $i3$ of the third model is determined using assumptions.
On the uniform placement of the intensity of the mass μ_K within the area of the body of the electric locomotive.

$$i_3 = \mu_3 \cdot \sqrt{0{,}25^2 + 0{,}25 \cdot S^2}.$$

For the VL-80 electric locomotive:

$$i_3 = \mu_3 \cdot \sqrt{0{,}25^2 + 0{,}25 \cdot S^2} = 6738 \cdot 0{,}25 \cdot \sqrt{1 + 2{,}116^2} = 3942 \text{ kg*m}$$

For electric locomotive KZ-4A:

$$i_3 = \mu_3 \cdot \sqrt{0{,}25^2 + 0{,}25 \cdot S^2} = 2611 \cdot 0{,}25 \cdot \sqrt{1 + 2{,}116^2} = 1528 \text{ kg*m}$$

The development of algorithms and numerical studies are carried out using the data. Consideration of this task includes the following materials [5, 6]:

- Algorithms for numerical studies of vibrations of an approximate model of an electric locomotive when moving in curves.
- Numerical studies of the oscillation model of an electric locomotive crew when moving in curved sections of the track.

The numerical research algorithm is compiled according to the block type, each of which solves certain tasks.

The calculation sequence according to the flowchart:

1st block.

- Input of initial data:
- Weight of the locomotive, $G_л$
- Body weight, $G_к$
- Unsprung weight of one wheelset, q
- The length of the locomotive between the axles of the couplers, $L_л$
- The distance between the first and fourth wheelset of the electric locomotive section, $l_к$
- Modulus of elasticity of the 1st kind, E
- Moment of inertia of the cross-sectional area, I
- Rigidity of the 1st and 2nd stages of spring suspension, $Ж_Г$ $Ж_К$.
- Ширина рельсовой колеи, S
- Rail clearance, Δ
- The distance between the sleepers , $l_ш$
- Number of sleepers per 1 km of track, $N_ш$
- The friction force of the sleeper on the gravel ballast, $f_ш$
- The resistance force of a single unloaded sleeper to its movement by 1 cm across the path, $N_{ШБ}$
- Radius of the curve of the track, R
- The speed of the electric locomotive, v

2nd Block

The basic parameters of the approximate model are calculated here. These include the intensities of the masses *μ1, μ2, μ3,* the mass moments of inertia *i1, i2, i3,* and the coupling intensities of the models. *K1, K2, K3.*

3rd Block

1 model of the IEE interaction between a locomotive wheel and a rail is calculated. Here, the force from the impact of the wheel on the rail is determined, as well as the contact stresses in the wheel-rail zone and the frequency of natural vibrations and the force from the impact of the 1st model on the second. There are 2 possible solutions based on the condition:

The first one $4\psi_1^{\,4} = \dfrac{k_1 - \mu_1 \cdot p_1^2}{EI_1} < 0$

The second one is when $4\psi_1^{\,4} < 0$

In the first case, two frequencies of natural resonant vibrations are obtained: the highest and the lowest, while in the second case only one lower frequency of vibrations is obtained.

The 4th block

Similarly to block 3, the parameters of the interaction of the bogie masses and the elastic rail track are calculated. As well as for the 3rd block, the solution depends on the coefficient 4ψ2, which determines the number of resonant frequencies of natural vibrations.

5th block

A block for calculating the model of interaction between the body masses of an electric locomotive and an elastic rail track.

The 6th block

Based on the formulas of claim 2, fluctuations in the ratio and wobble in the field of centrifugal forces are calculated.

The 7th block

Using the charting wizard, the necessary diagrams and tables of the obtained values of the oscillation parameters are constructed depending on the speed of movement and the radius of the curves of the track sections.

2. Results and Their Analysis

The main factors influencing the magnitude of the oscillations in the horizontal plane are the speed of the electric locomotive v, the radius of the curve R and the modulus of elasticity UG of the trackbed base in the horizontal plane. Numerical studies of the vibration parameters of the crew of the VL-80 and KZ-4A electric locomotives were carried out for the radii of curves 250, 400, 500, 600, 700 and 1000 m at speeds in the range of 60-100 km/h . The modulus of elasticity of the sub-rail base was assumed to be UG = 2.87 MPa, which corresponds to the average value of the elasticity of the track for various operating conditions of the railway track. Numerical studies were carried out to determine the following parameters: the frequencies of natural resonant vibrations, the maximum values of cutting forces, torque and bending stresses, as well as the magnitude of the oscillations of the ratio and wobble. The result is summarized in Tables 2-7.

Numerical studies show that each crew according to claim 2.1 is characterized by two frequencies of resonant natural vibrations: the highest and the lowest (Tables 2 and 3), each of these frequencies ij has its own characteristic dependence on the speed of movement v and the radius of the curve.

For the lower frequencies of resonant vibrations p_{12}, p_{22} and p_{32}, with a decrease in the radius of the curve, the frequency at which the resonance phenomenon is observed decreases and amounts to: for the first model, within 8.4 $\div$ 17.8 s^{-1} (VL80 electric locomotive) and 8.8 $\div$ 32.5 s^{-1} (KZ4A electric locomotive), for the second model, within 6.4 $\div$ 14.0 s^{-1} (electric locomotive VL80) and 5.3 $\div$ 21.1 s^{-1} (electric locomotive KZ4A) and for the third – 4.0 $\div$ 6.8 s^{-1} (electric locomotive VL80) 3.1 $\div$ 6.8 s^{-1} (electric locomotive KZ4A). This frequency range lies in the range of operating frequencies that occur when an electric locomotive is moving in a curve, which indicates the possibility of a sharp increase in the fluctuations of the locomotive crew when moving in a curve [7].

The values of the higher oscillation frequencies are within the limits: for the first model 185 $\div$ 205 s^{-1} (electric locomotive VL80) and 303 346 s^{-1} (electric locomotive KZ4A); for the second model 90 $\div$ 95 s^{-1} (electric locomotive VL80) and 117.5 $\div$ 125 s^{-1} (electric locomotive KZ4A) and for the third 70 $\div$ 79 s^{-1} (VL80 electric locomotive) and 91.2 $\div$ 96.4 s^{-1} (KZ4A electric locomotive). These oscillation frequencies are higher than the frequencies that occur in the crew of an electric locomotive in operation.

The analysis of the force loading (Table 4) of the rail track and the bandages shows that with increasing speed, the magnitude of the shearing force (Table 1) increases sharply and reaches 136.5 kN at a curve radius of 250 m and a speed of 90 km/h.

Table 2.
Frequencies of resonant vibrations of the VL-80S electric locomotive.

Radius of the curve, M	V, Km/H	Wheel Sets		Trolleys		Bodywork	
		P_{11}	P_{12}	P_{21}	P_{22}	P_{31}	P_{32}
R=250	60	197.3	12.9	93.1	9.9	74.7	5.5
	65	195.6	13.6	92.7	10.5	75.4	5.8
	70	193.8	14.4	92.3	11.1	76.0	5.9
	75	192.1	15.0	91.9	11.7	76.6	6.1
	80	190.4	15.7	91.5	12.2	77.1	6.3
	85	188.8	16.3	91.1	12.7	77.6	6.4
	90	187.2	16.8	90.8	13.2	78.0	6.5
	95	185.7	17.3	90.4	13.6	78.4	6.7
	100	184.2	17.8	90.0	14.0	78.7	6.8
R=400	60	201.6	10.7	94.1	8.2	72.7	4.8
	65	200.2	11.4	93.8	8.8	73.4	5.1
	70	198.9	12.1	93.5	9.3	74.0	5.3
	75	197.5	12.7	93.2	9.8	74.6	5.5
	80	196.2	13.4	92.9	10.3	75.2	5.7
	85	194.8	14.0	92.5	10.8	75.7	5.8
	90	193.4	14.5	92.2	11.3	76.2	6.0
	95	192.1	15.0	91.9	11.7	76.6	6.1
	100	190.7	15.5	91.6	12.1	77.0	6.3
R=600	60	204.3	9.0	94.7	6.9	71.1	4.2
	65	203.3	9.6	94.5	7.4	71.7	4.5
	70	202.3	10.3	94.3	7.9	72.3	4.7
	75	201.2	10.9	94.0	8.3	72.9	4.9
	80	200.2	11.5	93.8	8.8	73.4	5.1

	85	199.1	12.0	93.5	9.2	74.0	5.3
	90	197.9	12.6	93.3	9.7	74.4	5.4
	95	196.8	13.1	93.0	10.1	74.9	5.6
	100	195.7	13.6	92.8	10.5	75.3	5.7
R=700	60	205.2	8.4	94.9	6.4	70.6	4.0
	65	204.3	9.0	94.7	6.9	71.2	4.2
	70	203.4	9.6	94.5	7.3	71.7	4.4
	75	202.4	10.2	94.3	7.8	72.3	4.7
	80	201.4	10.8	94.1	8.2	72.8	4.9
	85	200.4	11.3	93.8	8.7	73.3	5.0
	90	199.4	11.8	93.6	9.1	73.8	5.2
	95	198.4	12.3	93.4	9.5	74.2	5.4
	100	197.4	12.8	93.1	9.9	74.7	5.5

Table 3.
Frequencies of resonant vibrations of electric locomotive KZ-4A.

Radius of the curve, m	**v, km/h**	**wheel sets**		**trolleys**		**bodywork**	
		p_{11}	p_{12}	p_{21}	p_{22}	p_{31}	p_{32}
1	2	3	4	5	6	7	8
R=250	60	341.1	14.4	124.3	8.7	91.2	4.4
	70	338.2	16.6	123.9	10.1	92.9	4.8
	80	335.0	18.7	123.4	11.5	94.5	5.1
	90	331.5	20.8	122.8	12.8	95.8	5.4
	100	327.8	22.7	122.1	14.1	96.9	5.6
	110	323.9	24.6	121.5	15.4	97.8	5.8
	120	319.9	26.4	120.8	16.6	98.6	5.9
	130	315.8	28.0	120.0	17.8	99.2	6.0
	140	311.7	29.6	119.3	18.9	99.8	6.1
	150	307.5	31.1	118.5	20.1	100.3	6.2
	160	303.3	32.5	117.7	21.1	100.7	6.3
R=400	60	344.3	11.5	124.8	6.9	88.6	3.8
	70	342.4	13.4	124.5	8.0	90.2	4.2
	80	340.2	15.1	124.2	9.2	91.8	4.5
	90	337.9	16.9	123.8	10.3	93.1	4.8
	100	335.3	18.5	123.4	11.3	94.3	5.1
	110	332.6	20.2	123.0	12.4	95.4	5.3
	120	329.7	21.7	122.5	13.4	96.3	5.5
	130	326.7	23.3	122.0	14.4	97.1	5.6
	140	323.6	24.7	121.4	15.4	97.9	5.8
	150	320.5	26.1	120.9	16.4	98.5	5.9
	160	317.3	27.5	120.3	17.4	99.0	6.0
R=600	60	346.1	9.5	125.1	5.7	86.7	3.2
	70	344.8	11.0	124.9	6.6	88.1	3.6
	80	343.3	12.5	124.7	7.5	89.5	4.0
	90	341.7	14.0	124.4	8.4	90.8	4.3
	100	339.9	15.4	124.1	9.3	92.0	4.6
	110	337.9	16.8	123.8	10.2	93.1	4.8
	120	335.8	18.2	123.5	11.1	94.1	5.0
	130	333.7	19.6	123.1	12.0	95.0	5.2
	140	331.4	20.9	122.8	12.8	95.8	5.4
	150	329.0	22.1	122.4	13.7	96.5	5.5
	160	326.5	23.4	121.9	14.5	97.2	5.6
R=700	60	346.6	8.8	125.2	5.3	86.0	3.1
	70	345.5	10.2	125.0	6.1	87.4	3.4
	80	344.2	11.6	124.8	7.0	88.7	3.8
	90	342.8	13.0	124.6	7.8	89.9	4.1
	100	341.2	14.4	124.4	8.7	91.1	4.4
	110	339.5	15.7	124.1	9.5	92.2	4.6
	120	337.7	17.0	123.8	10.3	93.2	4.8
	130	335.8	18.3	123.5	11.1	94.1	5.0

	140	333.7	19.5	123.1	11.9	95.0	5.2
	150	331.6	20.7	122.8	12.7	95.7	5.4
	160	329.4	21.9	122.4	13.5	96.4	5.5

Table 4.
Values of the maximum shearing forces acting on the wheel when moving the VL-80 and KZ-4A electric locomotives in curves at Uг=2.87 MPa.

Type of locomotive	V, km/h	Radius of the curve R, m					
		250	400	500	600	700	1000
ВЛ-80	60	60697	37936	30349	25290	21678	15174
	65	71235	44522	35617	29681	25441	17809
	70	82616	51635	41308	34423	29506	20654
	75	94839	59275	47420	39516	33871	23710
	80	107906	67441	53953	44961	38538	26977
	85	121816	76135	60908	50757	43506	30454
	90	136569	85355	68284	56904	48774	34142
	95	-	95103	76082	63402	54344	38041
	100	-	105377	84302	70251	60215	42151
KZ-4A	60	51845	32403	25923	21602	18516	12961
	70	70567	44105	35283	29403	25202	17641
	80	92169	57606	46085	38404	32917	23042
	90	116652	72907	58326	48605	41661	29163
	100	144015	90009	72000	60006	51434	36004
	110	-	-	87129	72608	62235	43564
	120	-	-	-	86409	74065	51845
	130	-	-	-	-	86923	60846
	140	-	-	-	-	-	70567
	150	-	-	-	-	-	-
	160	-	-	-	-	-	-

This indicates that the level of force interaction between the wheel and the rail remains very high when moving in small-radius curves, which adversely affects the wear of both the bandages and the rails [8, 9]. Therefore, the task of reducing dynamic forces when moving a locomotive in a curve remains relevant. The range of forces acting on the crew in the curve is in the range of 20-130 kN, which corresponds to experimental data obtained during train tests of the VL-80 electric locomotive. However, in the high-speed zone of 90 km/h and above, there is some difference between the results obtained and the field test data. The values of the maximum moments acting on the rail and bending stresses are shown in Table 5. The values of bending stresses reaching the order of 500 MPa, Table 6, indicate that the rail, when moving the locomotive in a curve, experiences complex loading in various planes, which adversely affects the rail track [10].

Table 5.
Values of the maximum moments acting on the rail when the VL80 electric locomotive is moving in curves at Uг =2.87 Mpa.

Type of locomotive	V, km/h	Radius of the curve R, m					
		250	400	500	600	700	1000
ВЛ-80	60	31202	19501	15601	13001	11144	7801
	65	36619	22887	18310	15258	13078	9155
	70	42470	26543	21235	17696	15168	10617
	75	48753	30471	24377	20314	17412	12188
	80	55470	34669	27735	23113	19811	13868
	85	62621	39138	31310	26092	22365	15655
	90	70205	43878	35102	29252	25073	17551
	95	-	48889	39111	32592	27936	19555
	100	-	54170	43336	36114	30954	21668
KZ-4A	60	26651	16657	13326	11105	9518	6663
	70	36276	22672	18138	15115	12956	9069
	80	47381	29613	23690	19742	16921	11845
	90	59966	37479	29983	24689	21416	14991
	100	74033	46270	37016	30847	26440	18508
	110	-	-	44789	37324	31992	22395
	120	-	-	-	44420	38074	26652
	130	-	-	-	-	44684	31278
	140	-	-	-	-	-	36276
	150	-	-	-	-	-	41522

	160	-	-	-	-	-	47068

Table 6.
Values of the maximum bending stresses of the interaction of the wheel and rail during the movement of the VL-80 electric locomotive in curves at Ur = 2.87 Mpa.

Type of locomotive	V, km/h	Radius of the curve R, m					
		250	400	500	600	700	1000
ВЛ-80	60	208	130	130	87	74	52
	65	244	153	153	102	87	61
	70	283	177	177	118	101	71
	75	325	203	203	135	116	81
	80	370	231	231	154	132	92
	85	417	261	261	174	149	104
	90	468	293	293	195	167	117
	95	-	326	326	217	186	130
	100	-	361	361	241	206	144
KZ-4A	60	178	111	89	74	63	44
	70	242	151	121	101	86	60
	80	316	197	158	132	113	79
	90	400	250	200	167	143	100
	100	494	308	247	206	176	123
	110	-	-	299	243	213	149
	120	-	-	-	296	254	178
	130	-	-	-	-	198	209
	140	-	-	-	-	-	242
	150	-	-	-	-	-	277
	160	-	-	-	-	-	314

Table 7 shows the values of the oscillation amplitudes of the Y_i ratio and the wiggle of the φ_i crew. The magnitude of the ratio is more affected by an increase in the speed of movement, since the level of forces determining the lateral displacement of the crew is proportional to the square of the speed. Analysis of fluctuations in the body ratio shows that their magnitude is much higher than the ratio of the bogie frame, therefore, when upgrading the VL-80 electric locomotive, measures are envisaged to change the design of the 2nd stage of the spring suspension in order to improve the dynamic qualities and increase the reliability of the electric locomotive.

The analysis of waggle fluctuations shows that their level is low, which is typical for all locomotives with an axial formula of 2_0-2_0 and indicates that they fit better into curves than locomotives with an axial formula of 3_0-3_0.

Table 7.
Fluctuations in the ratio and wagging of the VL-80 type electric locomotive model when moving in curved sections of the track.

R	V	φ_1	φ_2	φ_3	Y_1	Y_2	Y_3
m	m/s	rad	rad	rad	m	m	m
R=250	60	-0.010	-0.036	-0.025	0.005	0.022	0.025
	65	-0.015	-0.054	-0.044	0.005	0.023	0.028
	70	-0.018	-0.067	-0.062	0.005	0.024	0.031
	75	-0.020	-0.076	-0.079	0.005	0.024	0.034
	80	-0.021	-0.083	-0.097	0.005	0.025	0.037
	85	-0.022	-0.089	-0.115	0.006	0.026	0.040
	90	-0.022	-0.093	-0.134	0.006	0.027	0.044
	95	-0.022	-0.096	-0.152	0.006	0.028	0.048
	100	-0.022	-0.099	-0.172	0.006	0.028	0.052
R=400	60	0.006	0.025	0.019	0.004	0.021	0.019
	65	0.002	0.008	0.006	0.004	0.021	0.021
	70	-0.001	-0.006	-0.006	0.005	0.022	0.023
	75	-0.004	-0.017	-0.018	0.005	0.022	0.025
	80	-0.006	-0.026	-0.031	0.005	0.023	0.027
	85	-0.007	-0.033	-0.044	0.005	0.023	0.029
	90	-0.008	-0.039	-0.057	0.005	0.024	0.031
	95	-0.009	-0.043	-0.070	0.005	0.024	0.034
	100	-0.010	-0.047	-0.084	0.005	0.025	0.036
R=500	60	0.010	0.044	0.033	0.004	0.020	0.018
	65	0.006	0.026	0.022	0.004	0.021	0.019
	70	0.003	0.012	0.012	0.004	0.021	0.020

	75	0.000	0.001	0.001	0.004	0.021	0.022
	80	-0.002	-0.008	-0.009	0.005	0.022	0.023
	85	-0.003	-0.015	-0.020	0.005	0.022	0.025
	90	-0.004	-0.021	-0.031	0.005	0.023	0.027
	95	-0.005	-0.026	-0.043	0.005	0.023	0.029
	100	-0.006	-0.030	-0.054	0.005	0.024	0.031
R=700	60	0.014	0.065	0.050	0.004	0.020	0.015
	65	0.010	0.047	0.041	0.004	0.020	0.016
	70	0.007	0.033	0.033	0.004	0.020	0.017
	75	0.004	0.022	0.025	0.004	0.021	0.018
	80	0.003	0.013	0.016	0.004	0.021	0.020
	85	0.001	0.006	0.008	0.004	0.021	0.021
	90	0.000	-0.001	-0.001	0.004	0.022	0.022
	95	-0.001	-0.006	-0.010	0.005	0.022	0.024
	100	-0.002	-0.010	-0.019	0.005	0.022	0.025

2.1. Vertical Impact of the KZ4A Locomotive on the Track Superstructure

Analysis of the graphs in Figure 5 shows that at high speeds the rail deflection does not exceed the permissible value (6 mm). This is explained by the fact that under the action of several wheels, the deflections from adjacent wheels reduce the overall deflection. In addition, at high speeds the gyroscopic effect appears. The rail does not have time to deflect much under the action of the wheels, and thus the time of action of the wheels on the rail is reduced. This reduces the deflection of the rail under the action of high-speed vehicles.Таким образом, можно сделать следующий вывод.

The railway track allows the operation of high-speed two-axle vehicles at speeds of up to 180 km/h, provided that the track is maintained in good technical condition. If there are deviations in the track maintenance (various unevennesses), they will cause additional impact effects, which leads to the need to limit the speed of movement [11].

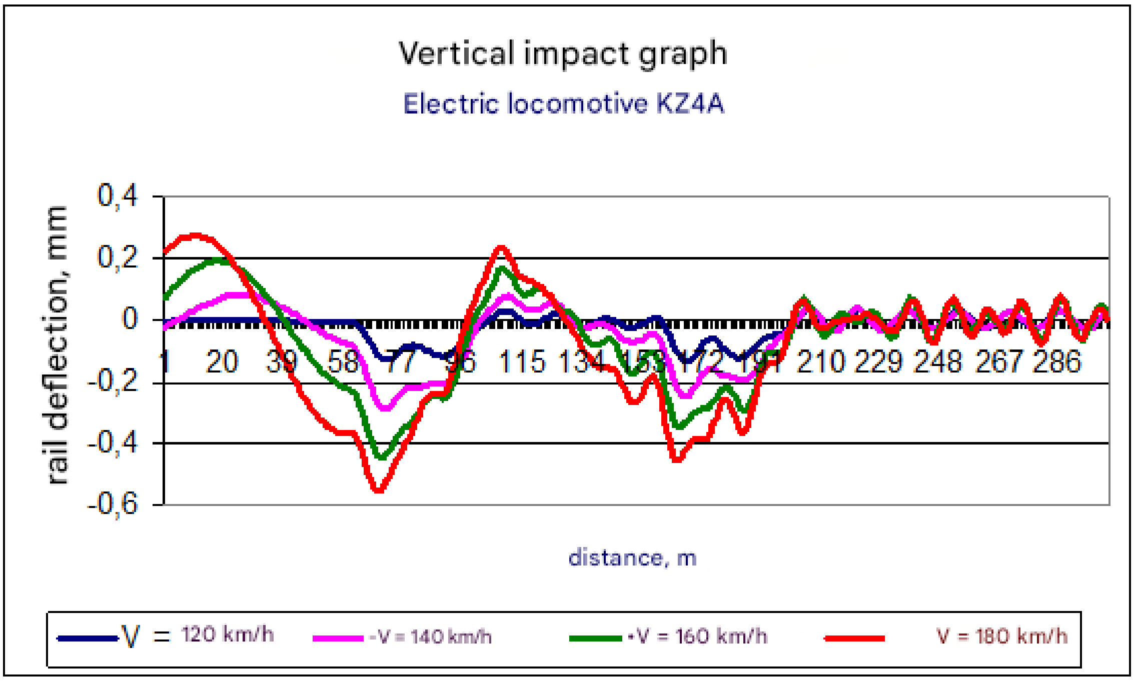

Figure 5.
Vertical impact graph.

It is evident from Figure 6 that the rail under the wheel has a deflection of a smaller magnitude than in the section behind the wheel. The lag of vertical deflections in relation to the acting load can occur not only as a result of inelastic resistance proportional to the deflections, but also proportional to the speed of vertical oscillations [12].

The deflection diagram turns out to be asymmetrical, and the wheel moving along the path is as if on an incline (Figure 6). The effect of dissipative forces is more pronounced the higher the speed of movement.

The design parameters of the rolling stock have a significant impact on the strength and stability of the railway track. As the speed of trains increases, additional dynamic forces of interaction between the track and the rolling stock arise [13].

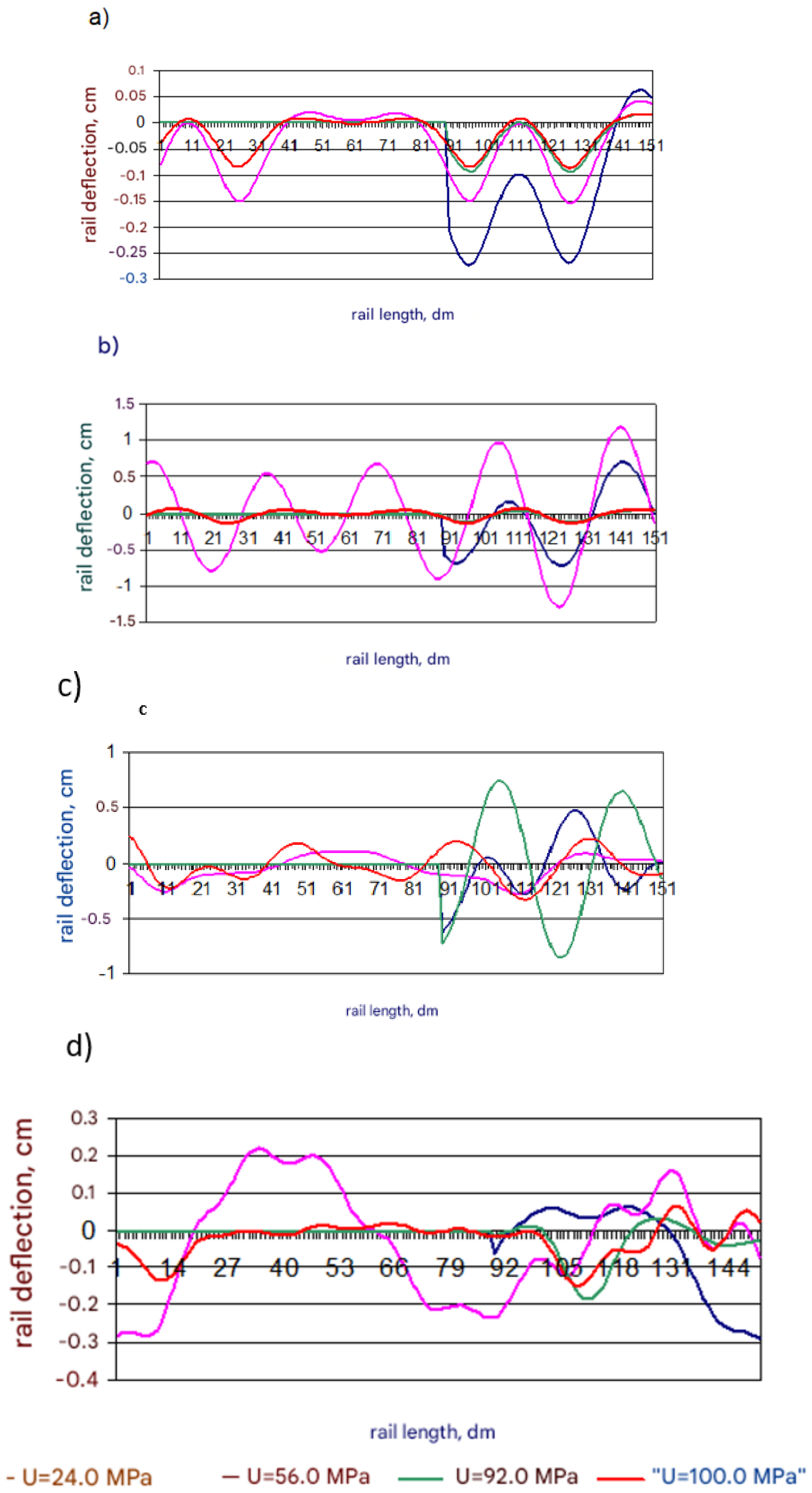

a) for a speed of 40 km/h; b) for a speed of 60 km/h;
c) for a speed of 80 km/h; d) for a speed of 100 km/h

Figure 6.
Rail deflection graphs from the KZ4A electric locomotive.

2.2. Vertical Impact of the VL-80 Locomotive on the Track Superstructure

The classical theory of vertical interaction of the track and the vehicle is based on the assumption that the rail deflection line is identical to the dynamic and static loads. It is generally accepted that elastic deformations occur instantly under the action of applied dynamic forces. In this case, the wave nature of elastic wave propagation is not taken into account. At high speeds, such an assumption can lead to errors in calculations, given that several vehicle wheels simultaneously affect the rail and the wave nature of elastic deformation propagation [14].

When deriving the equation of rail oscillations, it is necessary to take into account the forces of inelastic vertical resistance developing under load, which can manifest themselves as friction forces independent of vertical loads, and as forces representing the vertical component of oscillation velocities. It is also necessary to take into account the inertia force of rotation of the beam section.

Increased speeds lead to an increase in the magnitude of the waves that occur in front of the first wheel of the bogie. The maximum deflection of the rail in front of the wheel reaches a value of up to 0.7 mm. Then the absolute deflection of the rail will be 2.6 mm. Frequent changes in the sign of the rail bend in front of the wheel increase the stress state of the rail and can negatively affect the safety of train traffic. These waves can cause wave-like wear of the rail, since when moving along it, the wheels wear out the sections of the rail with a positive deflection more. In summer, rail deflections, regardless of the speed, are greater than in winter conditions. However, at a speed of 100 km / h, the rail deflection decreases compared to a speed of 60 km / h. At a speed of 60 km / h.

In summer, a resonance phenomenon appears, which leads to a deterioration in the consequences of rail vibrations under the locomotive.

Processing the calculation results of the rail deflection from the VL80 locomotive made it possible to obtain numerical values of the maximum rail deflection (Figure 7). Analysis of Figure 7 showed that, depending on the season, there are two peaks of rail deflection. The first peak occurs at a speed of 60 km / h, which corresponds to the movement of the vehicle in the summer (the modulus of elasticity of the under-rail base was set within 24-56 MPa), the second peak - at a speed of 80 km / h, which corresponds to the movement of the vehicle in the summer (the modulus of elasticity of the under-rail base is 92-100 MPa). It follows from this that at speeds of 60 and 80 km / h, the impact of the rolling stock is most unfavorable, which is due to the coincidence of the rail deflection diagrams from the group of wheels of the rolling stock. However, there are reserves for increasing the speed. As a number of theoretical and experimental studies show, with an increase in speed, the vertical impact of the rolling stock on the track decreases (see Figure 7) [15, 16].

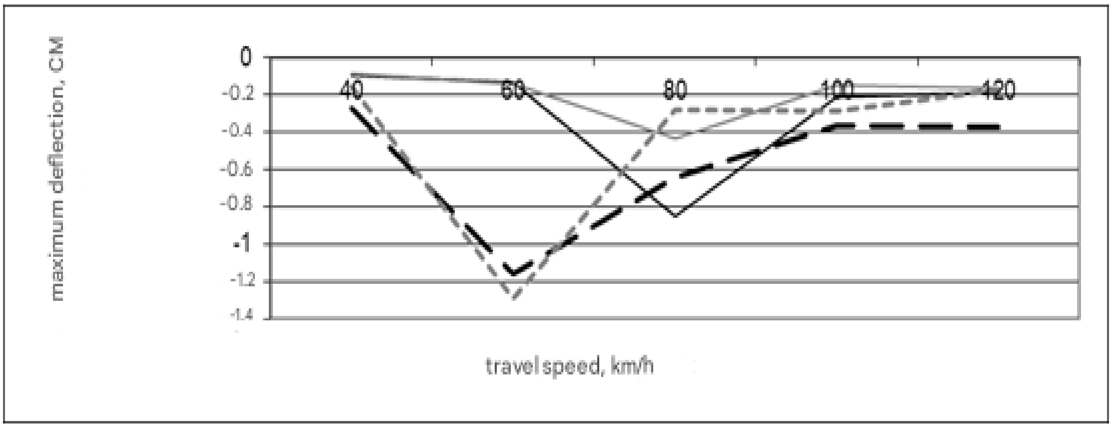

Figure 7.
Graphs of maximum rail deflections under the VL80 locomotive.

This phenomenon occurs due to the appearance of aerodynamic forces, a decrease in inertial forces acting on the rolling stock, and a gyroscopic effect.

The noted unloading of the wheels, which occurs with an increase in travel speeds, is predetermined by the interaction features of the track and the rolling stock. For freight locomotives and wagons, as shown by studies by the Central Research Institute of the Ministry of Railways, a decrease in wheel loads begins to be observed already when moving at a speed of 80 km / h on a track with reinforced concrete sleepers. It is noted that with an increase in the speed of an electric locomotive from 80 to 100 km / h, the intensity of growth of rail deflections decreases. The highest values of vertical rail deflections are recorded at a speed of 80 km / h. Using the technique, the influence of the main characteristics of the base part on the dynamic deflection of the rail is also considered. (See Figure 8).

The obtained rail deflection diagrams show that with an increase in the speed of movement, the rail deflection diagram loses its symmetry, there is a phenomenon of a delay in the maximum deflection relative to the movement of the wheel, a decaying wave appears in front of the vehicle, the length of which depends on the speed of movement of the vehicle [17]].

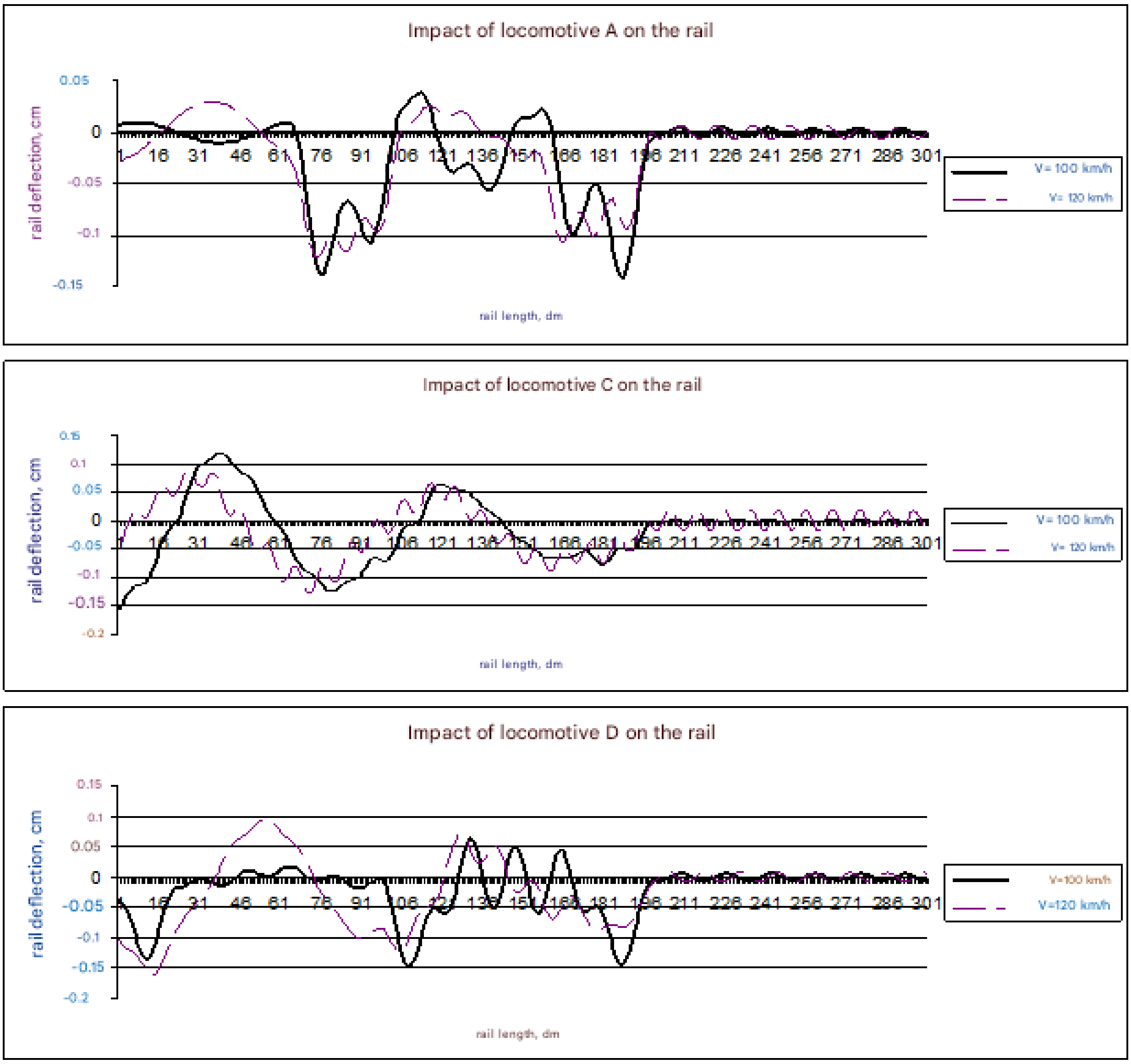

Figure 8.
Rail deflection graph.

3. Discussion of Dynamic Characteristics and their Impact on the Path

The developed method and algorithm for calculating the elastic deformations of a rail under the action of a multiaxial carriage can be used to determine the safe speeds of locomotives, depending on the modulus of elasticity of the sub-rail base and to optimize the parameters of the carriage [18].

The deflection of the rail is greatly influenced by the modulus of elasticity, the design of the railway track and the parameters of the running gear of the rolling stock [19-21].

As the speed of movement increases, the length of the rail subject to the oscillatory process increases. The amount of deflection of the rail is significantly affected by the number of axles of the rolling stock and the speed of movement. The use of two-axle trolleys helps to improve the interaction of the track and rolling stock, manifested in a decrease in the values of rail deflections [22].

The analysis shows that the VL-80 multi-heavy electric locomotive exhibits pronounced dynamic fluctuations at average speeds, due to the coincidence of the natural frequencies of the bogies and the body with the main excitation from the wheels at these speeds. Such resonant vibrations can cause local rail overloads and lead to contact fatigue failures if the condition of the track is not monitored [23]. The KZ4A is characterized by a different situation: at high speeds, kinetic energy is transferred more smoothly, which reduces the dynamic load on the rail. However, at low speeds, the KZ4A may experience fluctuations in the low frequency range (3-6 Hz), which coincide with the frequencies of path irregularities, which requires attention when driving along curves [24].

The force of the wheel–rail interaction increases with increasing speed only up to a certain threshold, after which aerodynamic effects and dynamic unloading limit the further growth of deflections. This effect is beneficial for the track: when switching to high-speed traffic, the peaks of dynamic loads shift to the region of high frequencies, which have little effect on the monolithic rigidity of the reinforced concrete track. At the same time, the "phase shift" of the deflections relative to the wheel indicates the presence of a viscous (dissipative) component of the elastic reaction of the track. Such an asymmetry of the plot (the wheel "rides up to the slide" on the rail) additionally dampens impacts, which is generally favorable [16, 25].

4. Conclusion

The main technical requirements for high-speed locomotives can be formulated from the following basic provisions:

a) compliance with train safety requirements;

b) improving the operating conditions of locomotives, ensuring the necessary durability and reliability, as well as the lowest maintenance and repair costs;

c) the need to maximize the reduction of the structure's own weight and economical metal consumption;

d) unification of the design through the use of standard and standard parts and elements;

e) Good dynamic and traction qualities.

Optimal design solutions for the mechanical part of traction rolling stock:

- The design of a passenger electric locomotive should provide for a support frame suspension of traction motors to the trolley frame with the transmission of torque to the wheelset using a hollow shaft and a one-way gear train).
- Trolley frames should be made of welded high-strength, low-alloy quiet steels, allowing their operation at low air temperatures with high reliability and weight reduction.
- Install vertical and transverse hydraulic vibration dampers between the trolley frame and the body, as well as a lateral vibration dampener, to ensure the necessary dynamic performance within the permissible driving speeds.
- Install speed and temperature monitoring sensors for axle box bearings and traction motors on the wheelsets, as well as grounding for current flow.
- The design of traction trolleys should not provide for oil addition sites in all pivots and in the spring suspension system.
- A high-speed locomotive must have a two-stage spring suspension. The total static deflection of the suspension spring must be at least 100 mm for freight, at least 140 mm for low-speed passenger and at least 180 mm for high-speed locomotives. The axial load should not exceed 25 t/axle.
- Appropriate damping devices (hydraulic and pneumatic) must be used to dampen vertical and horizontal vibrations.
- The wheelsets of two-axle trolleys and the outermost wheelsets of three-axle trolleys must have a free running range of at least 15 mm per side. For passenger locomotives, the lateral run-up of the bogie relative to the body should be within ± 40 mm. The axle boxes must be leashed.
- high-speed passenger locomotives should have a support frame suspension of traction electric motors. The use of such a traction motor suspension provides increased reliability and durability of the wheel-motor unit and less impact on the track.
- high-speed locomotives should not cause overvoltage in the elements of the upper structure of the track. The maximum speed should be limited by the conditions of stability of the railway track in straight and curved sections, such as the stability of the wheel against derailment, the stability of the track against a shift in plan, the stability of the track along the track width, the lateral stability of the carriage from overturning in the curve, the amount of outstanding acceleration.

Also, in the course of the research work, the following was established:

1. A mathematical model has been developed for the oscillation of a rail as a beam of infinite length lying on a continuous elastic base under the action of a group of vertical forces. This model allows you to determine the outline of the deflection of the rail under the action of several carriage wheels, taking into account the mutual influence of neighboring wheels on the bending moment of the rail.

2. When calculating the forces of interaction between the railway track and the rolling stock, it is necessary to consider the impact of all wheels of the rolling stock, since adjacent wheels affect the deflection of the rail.

3. When moving along the rail of a vertical load system at a speed of up to 40 km/h, the outline of the rail deflection plot is similar to the outline of the rail plot under static load. The obtained diagrams of the deflections of the rail show that as the speed of movement increases, the diagram of the deflection of the rail loses its symmetry, there is a phenomenon of a delay in the maximum deflection relative to the movement of the wheel, a damping wave appears in front of the crew, the length of which depends on the speed of movement of the crew. The deflection of the rail is greatly influenced by the modulus of elasticity, the design of the railway track and the parameters of the running gear of the rolling stock.

4. As the speed of movement increases, the length of the rail subject to the oscillatory process increases. This leads to an increase in the reduced mass of the track involved in the "wheel-path" oscillatory process. The reduced mass, taking into account the longitudinal vibrations of the rail, increases by 25-30% of the reduced mass of vertical vibrations of the track.

5. The most unfavorable speeds for railway tracks with a traditional design (rail, sleeper, ballast and roadbed) are speeds of 60 km/h in summer and 80 km/h in winter. At these values of the locomotive's speed, there is a sharp increase in rail deflections. This phenomenon is explained by the resonance caused by the coincidence of the oscillation amplitudes of the rail under adjacent wheels. With a further increase in the speed of movement, the deflection decreases compared to the deflection that occurs at resonant speeds. Based on this, it is recommended to operate electric locomotives with speeds close to the design speed, which gives an economic effect expressed in the intensification of the transportation process and in reducing the cost of the current maintenance of the railway track.

6. The amount of deflection of the rail is significantly affected by the number of axles of the rolling stock and the speed of movement. The use of two-axle bogies helps to improve the interaction of the track and rolling stock, manifested

in a decrease in the values of rail deflections, in reducing the lateral impact on the track and in reducing the wear of wheel ridges, and in a slight increase in the traction properties of locomotives.

References

[1] G. Kouroussis, D. P. Connolly, and O. Verlinden, "Railway-induced ground vibrations–a review of vehicle effects," *International Journal of Rail Transportation,* vol. 2, no. 2, pp. 69-110, 2014. https://doi.org/10.1080/23248378.2014.897791

[2] W. Zhai, K. Wang, and C. Cai, "Fundamentals of vehicle–track coupled dynamics," *Vehicle System Dynamics,* vol. 47, no. 11, pp. 1349-1376, 2009. https://doi.org/10.1080/00423110802621561

[3] T. Dahlberg, "Vertical dynamic train–track interaction: Verifying a theoretical model by full-scale experiments," *Vehicle System Dynamics,* vol. 40, no. 1-3, pp. 171–184, 2003.

[4] X. Lei and L. Mao, "Dynamic response analyses of vehicle and track coupled system on track transition of conventional high speed railway," *Journal of Sound and Vibration,* vol. 271, no. 3-5, pp. 1133-1146, 2004. https://doi.org/10.1016/S0022-460X(03)00570-4

[5] Z. W. Wang, M. X. Zhu, Y. Q. Xiang, and F. Li, "Development of a three-dimensional train–track interaction model using multibody dynamics and finite element methods," *Proceedings of the Institution of Mechanical Engineers, Part K: Journal of Multi-body Dynamics,* vol. 235, no. 2, pp. 379–393, 2021.

[6] J. C. Nielsen and X. Li, "Railway track geometry degradation due to differential settlement of ballast/subgrade–Numerical prediction by an iterative procedure," *Journal of Sound and Vibration,* vol. 412, pp. 441-456, 2018. https://doi.org/10.1016/j.jsv.2017.10.005

[7] E. Andersson and T. Dahlberg, "Vehicle–track dynamics in the mid-frequency range," *Vehicle System Dynamics,* vol. 30, no. 3-4, pp. 303–324, 1998.

[8] Y. Sun, M. Dhanasekar, and D. P. Thambiratnam, "Impact vibration behavior of railway vehicles due to rail surface irregularities," *Engineering Structures,* vol. 222, p. 111091, 2020.

[9] P. A. Montenegro, R. Calçada, A. A. Shvets, and D. Tokarev, "The effect of the evolution of rail surface defects on the wheel-rail contact forces and vehicle-track dynamics," *Proceedings of the Institution of Mechanical Engineers, Part F: Journal of Rail and Rapid Transit,* vol. 237, no. 5, pp. 665–679, 2023.

[10] J. N. Varandas, P. Holscher, and M. A. G. Silva, "Dynamic behavior of railway tracks on transitions zones," *Computers and Geotechnics,* vol. 76, pp. 114–124, 2016.

[11] A. M. Kaynia, C. Madshus, and P. Zackrisson, "Ground vibration from high-speed trains: Prediction and countermeasure," *Journal of Geotechnical and Geoenvironmental Engineering,* vol. 126, no. 6, pp. 531-537, 2000. https://doi.org/10.1061/(ASCE)1090-0241(2000)126:6(531)

[12] G. Lombaert, G. Degrande, and D. Clouteau, "Numerical modelling of free field traffic-induced vibrations," *Soil Dynamics and Earthquake Engineering,* vol. 19, no. 7, pp. 473-488, 2000. https://doi.org/10.1016/S0267-7261(00)00024-5

[13] D. P. Connolly, G. Kouroussis, O. Laghrouche, C. Ho, and M. Forde, "Benchmarking railway vibrations–Track, vehicle, ground and building effects," *Construction and Building Materials,* vol. 92, pp. 64-81, 2015. https://doi.org/10.1016/j.conbuildmat.2014.07.042

[14] C. E. Powell, "The dynamic response of railway track to high frequency vertical excitation," *Journal of Sound and Vibration,* vol. 409, pp. 295–311, 2017.

[15] M. Issametova *et al.*, "Determination of residual stresses in 3D-printed polymer parts," *Polymers,* vol. 16, no. 14, p. 2067, 2024. https://doi.org/10.3390/polym16142067

[16] D. Li, J. Hyslip, T. Sussmann, and S. Chrismer, *Railway geotechnics*. Boca Raton, FL: CRC Press, 2015.

[17] J. Gao, W. Zhai, and Y. Guo, "Vertical dynamics of railway vehicle–track system with a coupled fastening failure," *Mechanical Systems and Signal Processing,* vol. 135, p. 106367, 2020.

[18] B. A. Palsson, "Optimal design of railway slab tracks," Doctoral Dissertation, Chalmers University of Technology, 2014.

[19] P. Wang, H. Xu, Z. Li, and J. Wang, "Dynamic performance of a coupled high-speed train and track system with a voided sleeper," *Mechanical Systems and Signal Processing,* vol. 171, p. 108911, 2022.

[20] L. Zhou and Z. Shen, "Dynamic analysis of railway ballast under high-frequency vibration using the discrete element method," *Granular Matter,* vol. 21, no. 3, p. 64, 2019.

[21] C. Tang, X. He, P. Wang, and S. Yang, "Effect of unsupported sleepers on the dynamic response of the heavy-haul railway track," *Construction and Building Materials,* vol. 302, p. 124395, 2021.

[22] S. Abdullayev, G. Bakyt, A. Kamzina, N. Suleyeva, and N. Tokmurzina-Kobernyak, "Dynamic interaction of the TE-33A diesel locomotive and the track in a curve with a radius of 600 meters," *International Journal of Mechanical Engineering and Robotics Research,* vol. 13, no. 2, pp. 205-212, 2024. https://doi.org/10.18178/ijmerr.13.2.205-212

[23] J. Xiao, X. Zhang, and H. Li, "Dynamic response of the train–track–bridge system under seismic loads," *Engineering Structures,* vol. 177, pp. 652–666, 2018.

[24] I. Bondar, S. Abdullayev, A. Tursynbayeva, A. Abdullayeva, Y. Auyesbayev, and A. Izbairova, "Identifying The stress-strain state of railroad overpass Spans," *Eastern European Journal of Enterprise Technologies,* vol. 135, no. 7, pp. 14–28, 2025.

[25] S. Abdullayev, G. Bakyt, A. Kamzina, K. Sarsanbekov, and A. Abdullayeva, "Interaction of the TE33A diesel locomotive and the railway track on curved section with radius 290 m," *Communications – Scientific Letters of the University of Žilina,* vol. 25, no. 4, pp. B315–B326, 2023.